© 2016. Published by The Company of Biologists Ltd | Development (2016) 143, 4341-4351 doi:10.1242/dev.140970

Interplay between SOX7 and RUNX1 regulates hemogenic endothelial fate in the yolk sac

Andrew J. Lilly[1], Guilherme Costa[1,*], Anne Largeot[2], Muhammad Z. H. Fadlullah[1], Michael Lie-A-Ling[2], Georges Lacaud[2,‡] and Valerie Kouskoff[1,*,‡]

ABSTRACT

Endothelial to hematopoietic transition (EHT) is a dynamic process involving the shutting down of endothelial gene expression and switching on of hematopoietic gene transcription. Although the factors regulating EHT in hemogenic endothelium (HE) of the dorsal aorta have been relatively well studied, the molecular regulation of yolk sac HE remains poorly understood. Here, we show that SOX7 inhibits the expression of RUNX1 target genes in HE, while having no effect on RUNX1 expression itself. We establish that SOX7 directly interacts with RUNX1 and inhibits its transcriptional activity. Through this interaction we demonstrate that SOX7 hinders RUNX1 DNA binding as well as the interaction between RUNX1 and its co-factor CBFβ. Finally, we show by single-cell expression profiling and immunofluorescence that SOX7 is broadly expressed across the RUNX1$^+$ yolk sac HE population compared with SOX17. Collectively, these data demonstrate for the first time how direct protein-protein interactions between endothelial and hematopoietic transcription factors regulate contrasting transcriptional programs during HE differentiation and EHT.

KEY WORDS: SOX7, RUNX1, Hemogenic endothelium, Yolk sac, EHT

INTRODUCTION

Despite being the focus of intense research over recent years, the molecular mechanisms regulating the emergence of hematopoietic stem and progenitor cells (HSPCs) from hemogenic endothelium (HE) remains poorly understood. Clearly, this process of endothelial-to-hematopoietic transition (EHT) involves complex changes in gene expression that are regulated by an intricate balance of endothelial and hematopoietic transcription factors. It is now widely accepted that the hematopoietic transcription factor RUNX1 is a key master regulator of this process (Chen et al., 2009; Lancrin et al., 2009; Lie-A-Ling et al., 2014). RUNX1 is expressed in HE and emerging HSPCs both in the yolk sac and in the embryo proper (Frame et al., 2015; Lancrin et al., 2009; North et al., 1999), and controls the downregulation and upregulation of endothelial and hematopoietic transcriptional programs, respectively (Lancrin et al., 2012; Tanaka et al., 2012; Thambyrajah et al., 2016). RUNX1 has been shown to act in a heptad of interacting transcription factors in hematopoietic progenitor cells (HPCs) comprising FLI1, ERG, TAL1, LYL1, LMO2 and GATA2 (Wilson et al., 2010). Furthermore, it has been demonstrated that RUNX1 interacts with core binding factor β (CBFβ), which is thought to be key in enhancing RUNX1 binding to its DNA-binding sites, as well as enhancing RUNX1 protein stability (Huang et al., 2001; Link et al., 2010; Wang et al., 1993).

The SOXF family of transcription factors comprises SOX7, SOX17 and SOX18 (Bowles et al., 2000; Lilly et al., 2016; Wright et al., 1993). We and others have previously demonstrated that SOX7 is expressed in HE cells and its downregulation is necessary for the subsequent emergence of hematopoietic progenitors (Costa et al., 2012; Gandillet et al., 2009; Moignard et al., 2015). Therefore, SOX7 and RUNX1 appear to have contrasting effects in regulating opposing transcriptional programs in HE. Recent data have demonstrated that the interplay between SOX17 and RUNX1 regulates the emergence of HSPCs from the dorsal aorta (Bos et al., 2015; Lizama et al., 2015). It was further suggested that SOX17 binds to regulatory regions at the *Runx1* locus and inhibits *Runx1* expression, therefore maintaining endothelial identity of the arterial HE cells (Lizama et al., 2015). It was also proposed that, as HE differentiates, RUNX1 downregulates *Sox17* expression (Lizama et al., 2015). However, the molecular and biochemical details of the interaction between RUNX1 and SOX17 were not investigated.

Although the role of SOX17 in regulating the expression of RUNX1 has been demonstrated in arterial endothelial cells of the dorsal aorta at E10.5, its role in regulating the emergence of HPCs from the yolk sac has not been studied. HE is detected earlier in the yolk sac than in the dorsal aorta (from E8.5 to E9.5), and therefore arises before, during and after vascular remodelling (Frame et al., 2015). In contrast to the embryo proper, in the yolk sac HPCs emerge from a spectrum of endothelial cells in both arterial and venous regions, and in both large and small blood vessels (Frame et al., 2015). As the endothelial expression of SOX17 is restricted to arteries (Corada et al., 2013), this factor cannot control RUNX1 function and EHT in non-arterial vasculatures. Other endothelial transcription factors must therefore be important for regulating HE in the yolk sac. SOX7 is a prime candidate for this role, as previous studies have demonstrated that this SOXF factor is expressed from E7.5 in the yolk sac and is widely expressed in the developing vascular network: in both arteries and veins, and in large and small blood vessels (Gandillet et al., 2009; Sakamoto et al., 2007; Zhou et al., 2015).

Earlier studies have documented the interplay between SOX and RUNX factors. SOX9 and RUNX2 have been demonstrated to physically interact via their respective HMG and RUNT domains to regulate the differentiation of osteo/chondro progenitors (Akiyama

[1]Stem Cell Hematopoiesis, Cancer Research UK Manchester Institute, The University of Manchester, Manchester M20 4BX, UK. [2]Stem Cell Biology Group, Cancer Research UK Manchester Institute, The University of Manchester, Manchester M20 4BX, UK.
*Present address: The University of Manchester, Michael Smith Building, Oxford Road, Manchester M13 9PT, UK.

‡Authors for correspondence (valerie.kouskoff@manchester.ac.uk; georges.lacaud@cruk.manchester.ac.uk)

V.K., 0000-0001-9801-4993

Received 8 June 2016; Accepted 12 October 2016

Development (2016) 143, 4341-4351 doi:10.1242/dev.140970

et al., 2005; Zhou et al., 2006). SOX9 inhibits RUNX2 DNA binding and RUNX2 transcriptional activity, thereby promoting chondrogenesis; however, in progenitors expressing low levels of SOX9, RUNX2 is free to promote osteogenesis (Zhou et al., 2006). Therefore, the balance between the two factors regulates cell fate decisions that promote either osteogenesis or chondrogenesis (Zhou et al., 2006).

In this study, we show that enforced expression of SOX7 in HE inhibits the upregulation of the hematopoietic transcriptional program, including RUNX1 and TAL1 target genes. Surprisingly however, in contrast to what has been reported with SOX17, we found that SOX7 does not repress *Runx1* expression. We found that SOX7 inhibits the transcriptional activity of RUNX1 via direct protein-protein interactions through their respective HMG and RUNT domains, in a manner akin to that of SOX9 and RUNX2. Through this interaction, we show that SOX7 inhibits RUNX1 DNA binding, as well as its interaction with its pro-hematopoietic co-factor CBFβ. Finally, we demonstrate using immunofluorescence and single-cell qPCR profiling that SOX7 and RUNX1 are co-expressed in yolk sac HE at E8.5 and E9.5. Collectively, these data demonstrate for the first time how the balance between interacting endothelial and hematopoietic transcription factors regulates the dynamically changing transcriptional programs during HE differentiation and EHT.

RESULTS

SOX7 inhibits the expression of RUNX1 and TAL1 hematopoietic target genes in HE

In order to investigate the effect of SOX7 on hematopoietic gene expression in HE, we used a doxycycline-inducible *Sox7* (*iSox7*) ESC line, which was differentiated via embryoid body (EB) formation. FLK1^{+} cells sorted from *iSox7* EBs were cultured as a monolayer for 48 h to induce HE differentiation and cells were pulsed with doxycycline for 6, 12 and 24 h before harvesting and RNA-seq analysis (Fig. 1A). Principle component analysis (PCA) identified clear distinctions in the transcriptional programs of

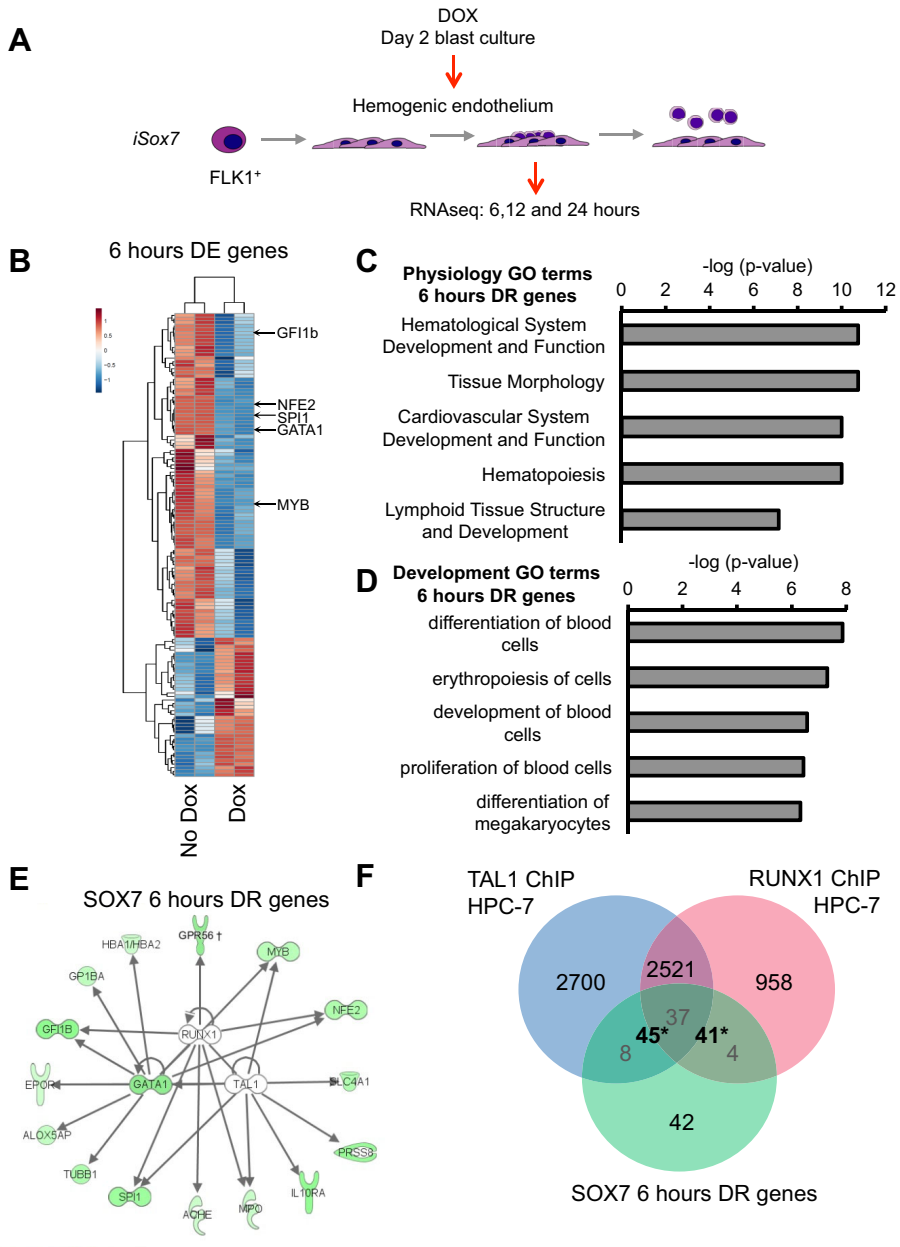

Fig. 1. SOX7 overexpression in HE suppresses a hematopoietic transcriptional program and inhibits the expression of RUNX1 and TAL1 target genes. (A) FLK1^{+} cells were sorted from day 3.5 *iSox7* EBs and cultured in HE differentiation media. Doxycycline (DOX) was added after 48 h, and RNA-seq was performed 6 and 12 h post-doxycycline induction. (B) A heatmap of 130 differentially expressed genes 6 h post-doxycycline induction. (C,D) Ingenuity pathway analysis of the genes suppressed by SOX7 at 6 h. (E) Ingenuity upstream analysis (IUA) of the genes suppressed by SOX7 at 6 h. Genes suppressed by SOX7 are indicated in green. GPR56 was not picked up in IUA, but has been shown to be regulated by RUNX1 (Solaimani Kartalaei et al., 2015). (F) Overlap between the genes suppressed by SOX7 at 6 h, with genes bound by RUNX1 and TAL1 in HPC-7 (HPC-7 ChIP dataset from Wilson et al., 2010). Asterisk indicates significance (RUNX1 overlap P-value=2.53×10^{-11}, TAL1 overlap P-value =4.79×10^{-8}, hypergeometric probability test).

Development (2016) 143, 4341-4351 doi:10.1242/dev.140970

untreated and doxycycline-treated cells at 6, 12 and 24 h (Fig. S1A). At 6 h post-doxycycline induction, 130 genes were differentially expressed. Of these, 91 genes were downregulated, including key hematopoietic transcriptional regulators such as: *Nfe2*, *Gfi1b*, *Spi1*, *Gata1* and *Myb* (Fig. 1B and Table S1). Ingenuity pathway analysis (IPA) of these genes identified a significant enrichment for hematopoietic GO terms such as: hematological system development and function, hematopoiesis, and development of hematopoietic cells (Fig. 1C,D). At 12 and 24 h post-doxycycline induction, 341 and 566 genes, respectively, were differentially expressed (Tables S2 and S3). Ingenuity pathway analysis (IPA) of the genes downregulated by SOX7 at 12 and 24 h again identified a significant enrichment for genes involved with hematopoietic GO terms (Fig. S1B,C; data not shown).

To examine whether these transcriptional changes following SOX7 enforced expression translate to functional changes in HE differentiation, FLK1$^+$ cells sorted from *iSox7* EBs were cultured as a monolayer for 48 h before treatment with and without doxycycline for 24 h. Cells were replated into hematopoietic progenitor cell CFU media with and without doxycycline and analysed after 8 days. Doxycycline treatment resulted in a decrease in the numbers of primitive and definitive hematopoietic colonies, whereas there was an expansion of poorly differentiated blast-like colonies, as previously described (Costa et al., 2012) (Fig. S1D). Harvesting the cells from the CFU assays identified that doxycycline treatment expanded the numbers of cells expressing the endothelial marker TIE2, while the numbers of CD45$^+$/CD41$^-$ hematopoietic cells decreased (Fig. S1E,F). These data, together with the RNA-seq data set, indicate that the enforced expression of SOX7 inhibits the full process of EHT.

In order to uncover the upstream positive regulators of the set of genes rapidly downregulated by SOX7 at 6 h, we further examined this gene set using ingenuity upstream analysis. RUNX1 and TAL1 were identified as upstream activators of these genes (Fig. 1E); the expression levels of RUNX1 and TAL1 themselves were not affected by SOX7-enforced expression. Furthermore, we observed that 53.8% of the genes downregulated by SOX7 at 6 h were bound by RUNX1 and/or TAL1 in HPC-7 hematopoietic progenitors, whereas 40.7% of the genes were bound by both RUNX1 and TAL1 (Fig. 1F). Collectively, these data indicate that in HE, SOX7 inhibits the expression of hematopoietic genes, many of which are direct transcriptional targets of RUNX1 and TAL1.

SOX7 and RUNX1 are co-expressed in HE of the yolk sac and dorsal aorta

Previous studies have suggested that SOX7 is expressed from the onset of endothelial differentiation in the yolk sac at E7.5, whereas SOX17 is expressed in developing arterial endothelium at later stages of development (Corada et al., 2013; Gandillet et al., 2009; Sakamoto et al., 2007). In order to define the expression of the three SOXF factors in yolk sac HE, we sorted FLK1$^+$/RUNX-RFP$^+$/CD41$^-$ HE cells from *Runx1-rfp* transgenic E8.5 embryos and performed single-cell qPCR. Substantial overlap for the expression of the three SOXF factors was evident; however, SOX7 was the most broadly expressed across the HE population: SOX7 was expressed in 80% of cells and 20% of cells expressed only SOX7 (Fig. 2A). This is in stark contrast to SOX17, which was expressed in fewer than 50% of HE cells (and as little as 4% of these cells expressed only SOX17). These data suggest that, in yolk sac HE, SOX7 is likely to be the most important SOXF factor regulating its development.

In order to further investigate SOX7 and RUNX1 co-expressed in yolk sac HE, we performed immunofluorescence for RUNX, SOX7 and PECAM1 in E8.5 and E9.5 embryos. RUNX staining in yolk sac at E8.5 showed similar patterns to proximal RUNX1-RFP expression (Fig. S2A,B), confirming previous studies demonstrating that RUNX1 is the prevalent RUNX factor expressed in the yolk sac at this stage of development (Landry et al., 2008; Otto et al., 1997). SOX7 was expressed in the yolk sac at E8.5, including in endothelial cells on the edges of blood island regions (Fig. S2B and Fig. 2B,C). RUNX expression was found mainly around the blood island regions, as previously described (Fig. S2B and Fig. 2B,C) (Frame et al., 2015). Importantly, and in agreement with our single-cell PCR analysis, we observed RUNX and SOX7 co-expressing endothelial cells on the edge of the blood island (Fig. 2B,C).

By E9.5, SOX7 was expressed throughout the yolk sac, but higher SOX7 expression was evident in endothelial cells of the larger blood vessels (Fig. S2C). At this stage after vascular remodelling, the blood islands disappear and RUNX is expressed in clusters throughout the yolk sac, as previously described (Fig. S2C) (Frame et al., 2015). RUNX and SOX7 co-expressing endothelial cells were more abundant than at E8.5, and these cells generally expressed lower levels of RUNX than cells in emerging hematopoietic clusters (Fig. 2D). SOX7 was also expressed in endothelial cells lining the dorsal aorta at E9.5, and endothelial cells co-expressing SOX7 and RUNX were clearly detected (Fig. 2E). Collectively, these data reveal that, in yolk sac HE, SOX7 is the predominant SOXF factor, whereas in the dorsal aorta it is likely that both SOX17 and SOX7 regulate the behaviour of HE. Furthermore, SOX7 and RUNX are found co-expressed in subsets of endothelial cells throughout development at sites of blood cell emergence.

SOX7 inhibits the differentiation of yolk sac HE

To investigate whether SOX7 also inhibits the expression of RUNX1 target genes *in vivo*, we analysed the expression of some of these targets in enriched yolk sac HE sorted on the FLK1$^+$/CD41$^-$ immuno-phenotype from E8.5 *Sox7*$^{+/+}$ and *Sox7*$^{-/-}$ embryos. QPCR analysis identified no change in the levels of RUNX1 transcripts, whereas there were significantly higher expression levels of *Nfe2*, *Myb* and *Spi1* in *Sox7*$^{-/-}$ cells (Fig. 3A). These data support the notion that SOX7 does not affect RUNX1 expression, but modulates the expression of potential RUNX1 target genes in yolk sac HE. In order to examine the role of SOX7 in regulating yolk sac HE differentiation *in vivo*, we isolated yolk sacs from E9.5 doxycycline-inducible *iSox7* or wild-type embryos, which were cultured either as explants or dissociated and cultured on OP9 cells (Fig. 3B). Doxycycline addition to *iSox7* yolk sac explant cultures resulted in a decrease in the number of CD45$^+$ hematopoietic cells compared with wild-type yolk sacs, indicating that the enforced expression of SOX7 inhibited the emergence of hematopoietic cells (Fig. 3C). In yolk sac dissociation cultures, SOX7-enforced expression expanded or maintained the TIE2$^+$/CD41$^+$ and TIE2$^+$/cKIT$^+$ HE populations compared with wild-type yolk sac cultures (Fig. 3D,E). Together, these data indicate that SOX7 inhibits the differentiation of HE and the subsequent emergence of hematopoietic progenitor cells.

SOX7 inhibits the transcriptional activity of RUNX1

The fact that SOX7 inhibits the expression of RUNX1 target genes, but not RUNX1 itself, suggested that SOX7 may inhibit the transcriptional activity of RUNX1 in a similar manner to that of

Development (2016) 143, 4341-4351 doi:10.1242/dev.140970

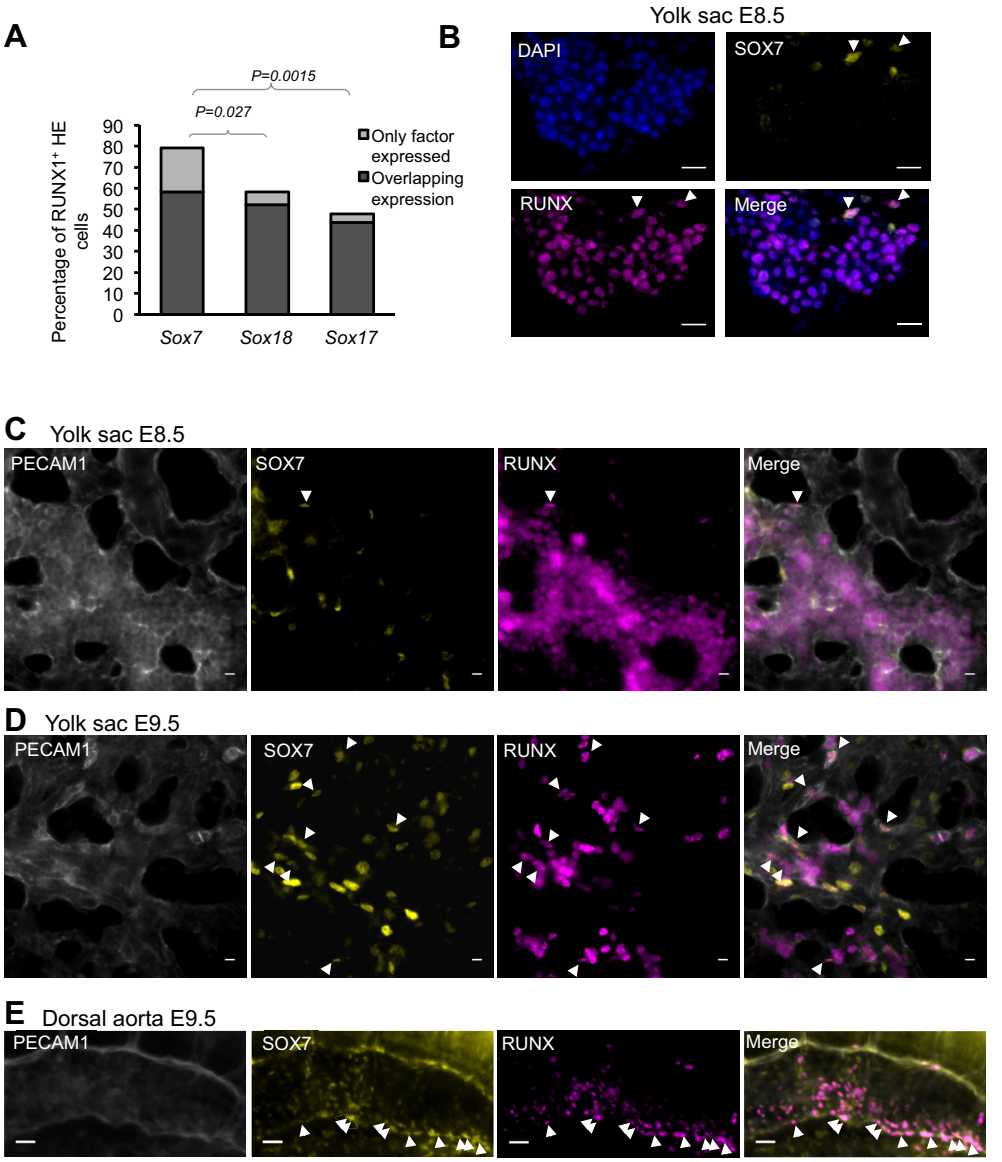

Fig. 2. SOX7 and RUNX1 are co-expressed in yolk sac hemogenic endothelium. (A) Single-cell qPCR on single sorted RUNX1-RFP^{+}/FLK1^{+}/CD41^{-} cells from E8.5 embryos. Data indicate the frequency of cells expressing *Sox7*, *Sox17* and *Sox18* (n=48 cells, chi-squared test). (B) Sections of blood island region at E8.5 stained for SOX7 and RUNX expression. Arrowheads indicate SOX7 and RUNX co-expressing cells. Scale bars: 20 µm. (C,D) Whole-mount staining of yolk sacs at E8.5 (C) and E9.5 (D). Scale bars: 10 µm. (E) Whole-mount staining of the dorsal aorta at E9.5. Scale bars: 50 µm. Arrowheads indicate RUNX and SOX7 co-expressing cells.

SOX9, which inhibits RUNX2 transcriptional activity during osteochondrogenic differentiation (Akiyama et al., 2005). To investigate this hypothesis, we performed transcriptional activity assays with the osteocalcin 6×OSE2-luc RUNX luciferase reporter. RUNX1 strongly activated the transcription of the reporter construct, but the addition of SOX7 completely inhibited this RUNX1-induced activation, with levels returning to baseline (Fig. 4A). The RNA-seq data presented above revealed that the hematopoietic transcriptional regulator *Nfe2* was rapidly downregulated upon doxycycline-induced SOX7 expression; furthermore, the promoter region of *Nfe2* has been shown previously to be bound by RUNX1 in hematopoietic progenitors (Goode et al., 2016; Wilson et al., 2010). Therefore, we cloned the NFE2 promoter region (−3562/+58 TSS) containing RUNX1 and FLI1 ChIP-seq peaks (Goode et al., 2016; Wilson et al., 2010) and performed transcriptional activity assays. The addition of RUNX1 and FLI1 individually produced minimal activation of the *Nfe2* promoter; however, when added together, a stronger activation was observed (Fig. 4B). The addition of SOX7 inhibited the activation of the *Nfe2* promoter by RUNX1 and FLI1, with levels returning to baseline (Fig. 4B). Deletion of two RUNX1-binding sites within the *Nfe2* promoter region abrogated the activation by RUNX1 and FLI1, confirming that the *Nfe2* promoter is directly activated by RUNX1 (Fig. 4C and Fig. S3).

In order to characterise the important domains of SOX7 that are required for its inhibitory effect on RUNX1 transcriptional activation, we performed mutagenesis of SOX7 followed by luciferase transcriptional analysis (Fig. 4D). Deletion of the HMG domain of SOX7 completely abrogated its inhibitory effects on RUNX1, whereas deletion of the transactivation domain had no effect (Fig. 4E). Furthermore, the R60E point mutation in the HMG domain reversed the inhibitory effect of SOX7 on RUNX1 (Fig. 4E). HMG domain deletion and the R60E mutation also abrogated the inhibitory effects of SOX7 on RUNX1 and FLI1 transcriptional activity at the *Nfe2* promoter region (Fig. 4F).

SOX7 and RUNX1 physically interact via their respective HMG and RUNT domains

The fact that SOX7 can inhibit RUNX1 transcriptional activity suggests that the two proteins can physically interact. To investigate this, we performed co-immunoprecipitation assays using HEK293T cells co-transfected with SOX7- and RUNX1-expressing plasmids.

Development (2016) 143, 4341-4351 doi:10.1242/dev.140970

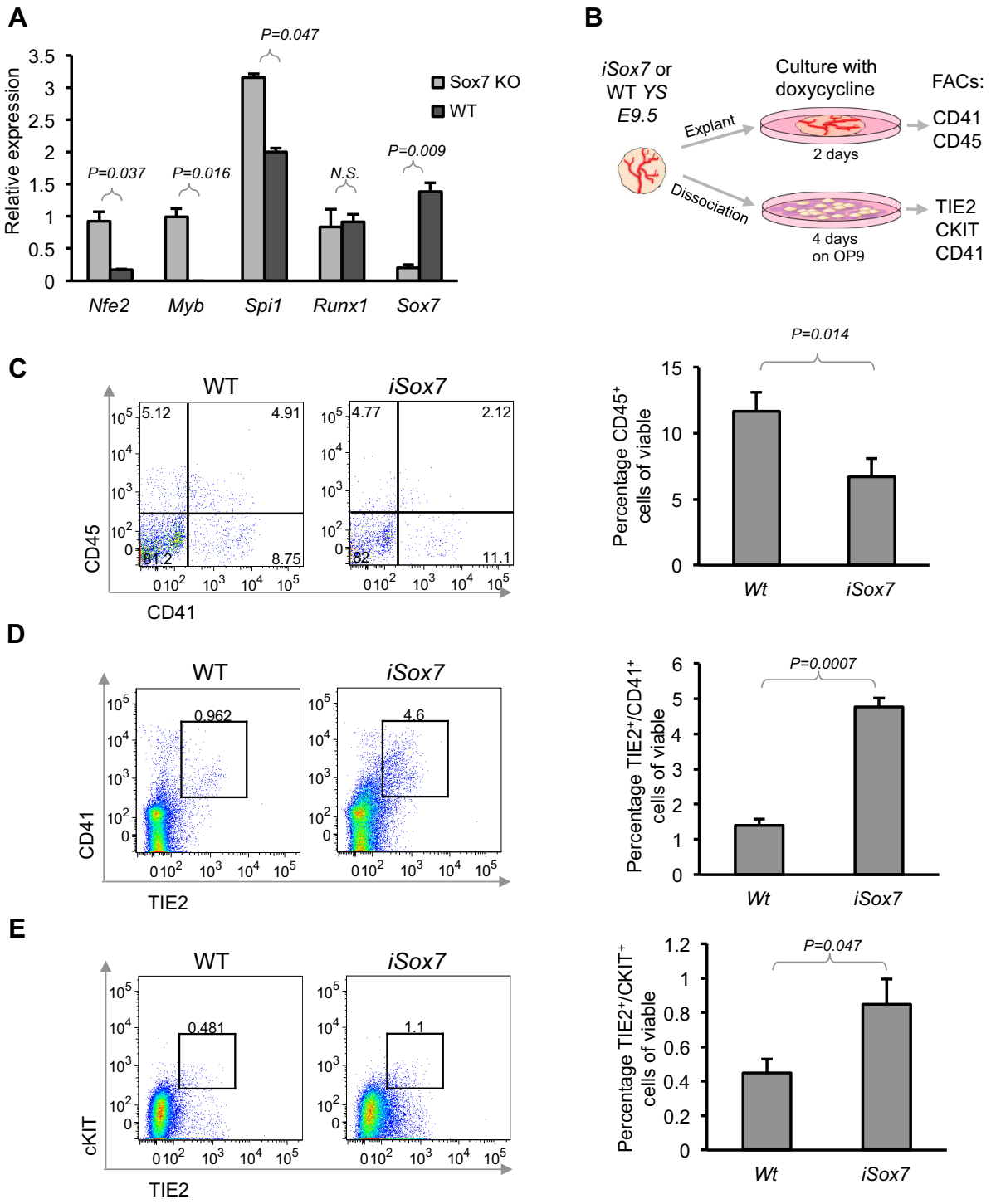

Fig. 3. SOX7 inhibits the differentiation of yolk sac HE. (A) qPCR on FLK1$^+$/CD41$^-$ cells from wild-type and SOX7 knockout (KO) embryos at E8.5. Data are presented as mean±s.e.m. from a pool of two embryos in each group (n=3 technical replicates) and analysed using Student's two-tailed t-test. (B) Yolk sacs from E9.5 *iSox7* or wild-type embryos were cultured with doxycycline either as explants for 2 days or dissociated and cultured on OP9 cells for 4 days before flow cytometry analysis. (C) Yolk sac explants were analysed for hematopoietic output (n=7 for wild type; n=6 for *iSox7* embryos). (D,E) Yolk sac dissociation cultures (n=6 for wild type; n=3 for *iSox7* embryos). (C-E, right panels) Data are presented as mean percentage of viable cell population±s.e.m. and analysed using Student's one-tailed t-test.

The subsequent isolation of SOX7 revealed that RUNX1 could be immunoprecipitated with SOX7 (Fig. 5A). The reverse experiment, pulling down RUNX1 and detecting SOX7, also showed that both proteins could be immunoprecipitated together (Fig. 5A), demonstrating that SOX7 and RUNX1 can physically interact.

In order to investigate further the interaction between SOX7 and RUNX1, we used Duolink proximity ligation assay (PLA) as a more-sensitive and quantitative method of assessing protein interactions, where each Duolink puncta represents a single protein-protein interaction. HEK293T cells were co-transfected

Development (2016) 143, 4341-4351 doi:10.1242/dev.140970

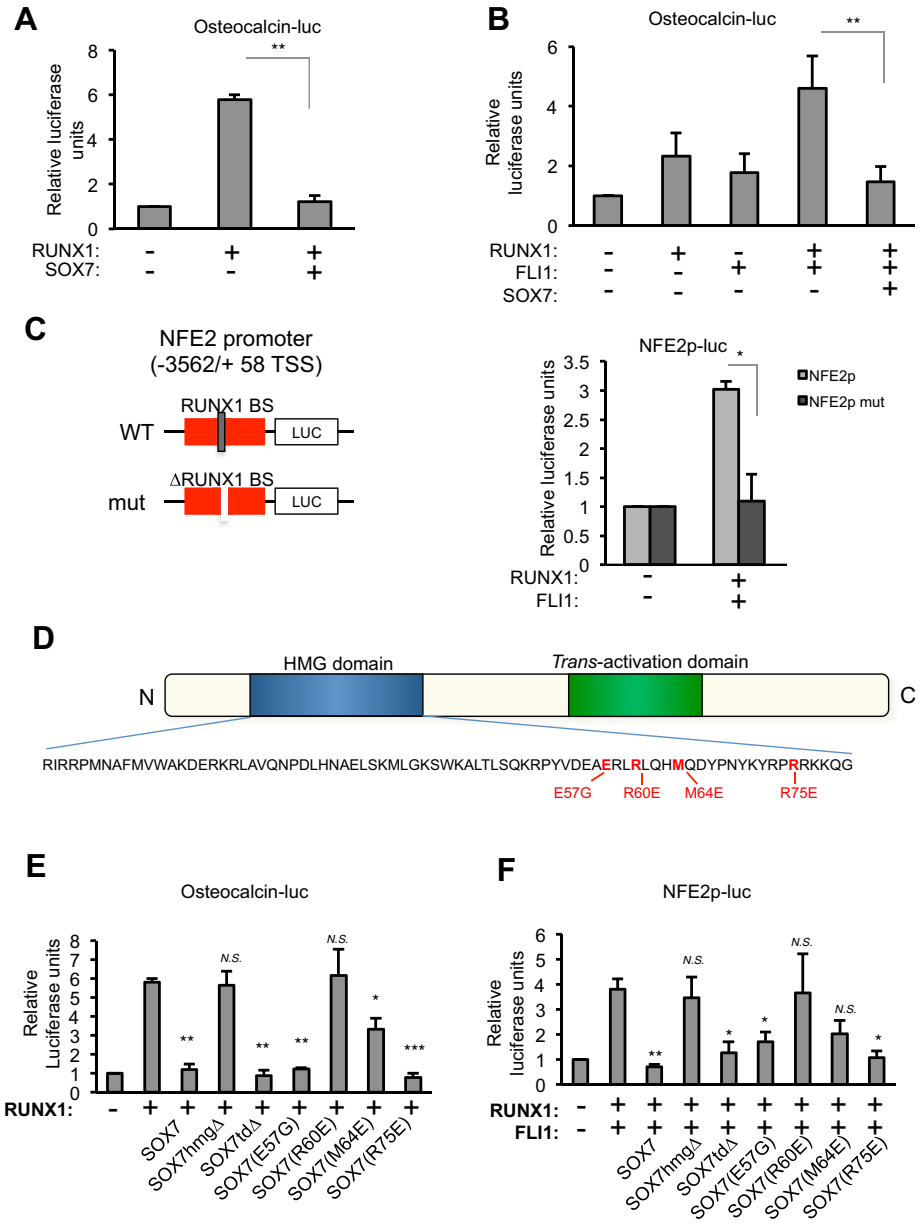

Fig. 4. SOX7 inhibits the transcriptional activity of RUNX1. (A,B) Luciferase analysis of the RUNX1 reporter (A) and the NFE2 promoter region (−3562/+ 58 TSS) (B). Data are presented as mean±s.e.m. (*n*=3 independent experiments) and analysed using Student's one-tailed *t*-test. (C) Deletion of RUNX1-binding sites in the NFE2 promoter (left panel) and luciferase analysis (right panel) (*n*=4 independent experiments analysed using Student's one-tailed *t*-test). (D) The structure of SOX7, amino acid point mutations in the HMG domain are indicated in red. (E,F) Luciferase analysis of SOX7 mutations on RUNX1 transcriptional activity at the RUNX1 reporter (E) and NFE2 promoter (F). Data are presented as mean±s.e.m. (*n*=3 and *n*=4 independent experiments) and are analysed using Student's one-tailed *t*-test.

with RUNX1- and SOX7-expressing plasmids before Duolink analysis. Duolink puncta were detected in cells transfected with wild-type RUNX1 and SOX7 plasmids, confirming an interaction between the two proteins (Fig. 5B,C and Fig. S4). However, deletion of the HMG domain of SOX7 or deletion of the RUNT domain of RUNX1 substantially decreased the number of Duolink puncta per cell, indicating a decrease in the interaction between RUNX1 and SOX7 (Fig. 5B,C and Fig. S4). Collectively, these data demonstrate that SOX7 and RUNX1 physically interact via their respective HMG and RUNT domains.

SOX7 inhibits RUNX1 interactions with CBFβ

The RUNT domain of RUNX1 provides key contacts for interacting with its co-factor CBFβ (Zhang et al., 2003), resulting in a RUNX1-CBFβ complex with much enhanced transcriptional activity. To test whether SOX7 can inhibit the interaction of RUNX1 with CBFβ, we performed a SOX7 competition assay using Duolink PLA. HEK293T cells were transfected with plasmids expressing FLAG-RUNX1 and HA-CBFβ, with or without untagged SOX7 competitor and a plasmid expressing GFP only (Fig. 6A). Transfected cells were enriched by sorting for GFP before Duolink PLA (Fig. 6A). Duolink puncta were detected between RUNX1 and CBFβ, as expected (Fig. 6B and Fig. S5). However, when untagged SOX7 was added at an equal concentration to RUNX1 and CBFβ, it resulted in a significant decrease in the number of Duolink puncta per cell between RUNX1 and CBFβ (Fig. 6B and Fig. S5A). Furthermore, the addition of untagged SOX7 at three times the concentration of RUNX1 and CBFβ completely abolished the interaction between RUNX1 and CBFβ (Fig. 6C and Fig. S5B). Deletion of the HMG domain of SOX7 significantly blunted the inhibitory effects of SOX7 on the interaction between RUNX1 and CBFβ, indicating that the HMG domain is important for this process (Fig. S6A,B). In the reverse experiment, CBFβ could outcompete SOX7 for RUNX1 binding, especially when CBFβ was added at three times the concentration of SOX7 and RUNX1 (Fig. S6C,D). These data therefore suggest that SOX7 and CBFβ compete for RUNX1 binding and that the balance between

Development (2016) 143, 4341-4351 doi:10.1242/dev.140970

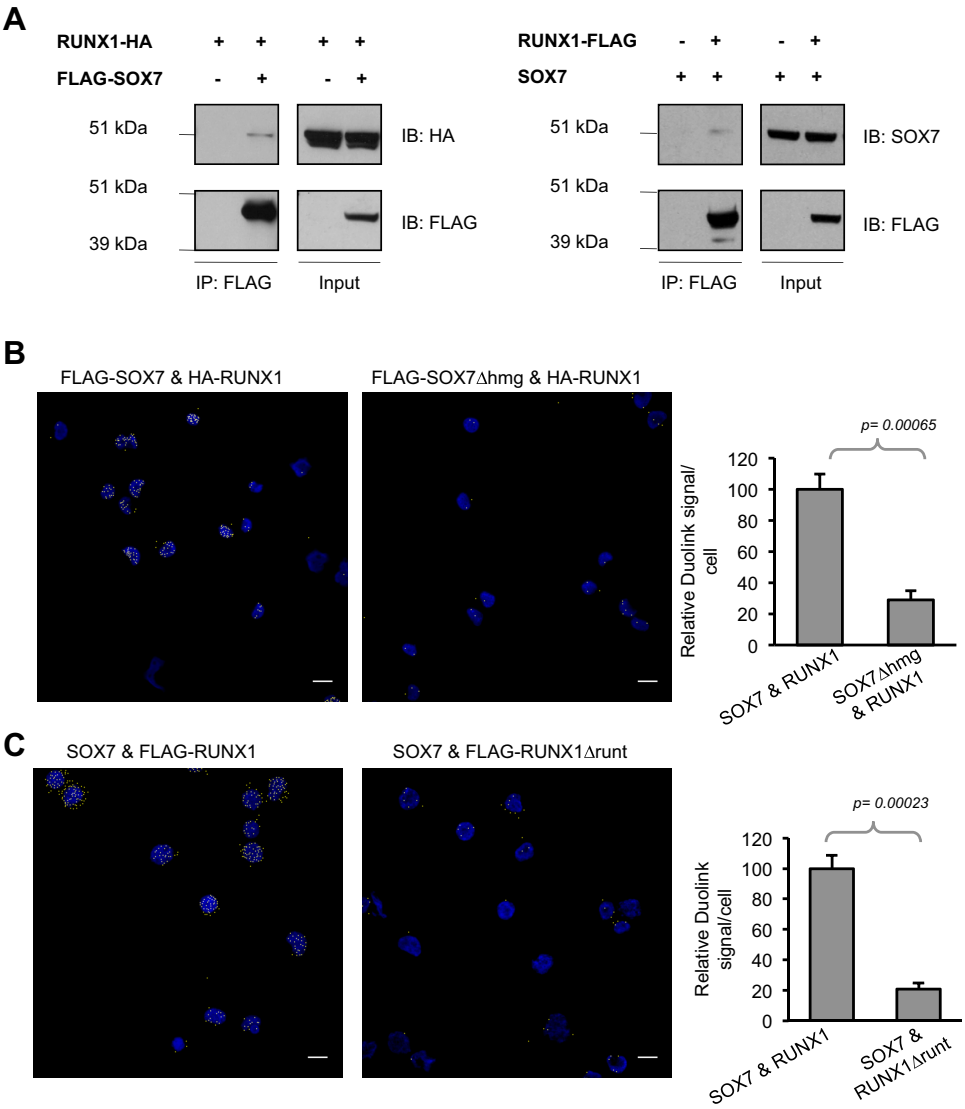

Fig. 5. SOX7 and RUNX1 physically interact via their respective HMG and RUNT domains. (A) Co-IP analysis of RUNX1 and SOX7. HEK293T cells were transfected with pcDNA3 plasmids expressing RUNX1 and SOX7 as indicated. Protein extracts were immunoprecipitated (IP) with anti-FLAG beads before immunoblot (IB) analysis. Data represent one of at least three independent experiments. (B,C) Duolink proximity ligation analysis (PLA) of SOX7 and RUNX1. HEK293T cells were transfected with the indicated pcDNA3 plasmids before PLA. Left panels: representative micrographs. Scale bars: 20 µm. Right panels: mean Duolink signal per cell±s.e.m. relative to wild-type SOX7 and RUNX1 (*n*=5 fields of view analysed using Student's two-tailed *t*-test).

these transcription factors could be important for regulating HE differentiation.

SOX7 inhibits RUNX1 binding to target DNA sites

As the RUNT domain is the DNA-binding domain of RUNX1, we investigated whether SOX7 can inhibit RUNX1 binding to its target DNA sites. FLK1$^+$ cells were isolated from day 3.5 *iSox7* EBs and reaggregated in HE differentiation media for 48 h. CD41$^+$ hematopoietic progenitor cells were isolated and cultured for a further 12 h with or without doxycycline to induce SOX7 expression. RUNX1 ChIP and analysis of the *Nfe2* promoter region identified enrichment for RUNX1 binding, which was significantly decreased upon SOX7 expression when the cells were cultured with doxycycline (Fig. 7A). To further investigate the effect of SOX7 on RUNX1 DNA binding, we performed a biotin-DNA-RUNX1 pull-down assay using nuclear extracts from *iSox7* CD41$^+$ cells cultured with or without doxycycline. The expression of SOX7 upon doxycycline addition resulted in a dramatic decrease in the amount of RUNX1 pulled-down by its DNA-binding site (Fig. 7B). Collectively, these data indicate that SOX7 inhibits the DNA-binding capacity of RUNX1.

DISCUSSION

In this study, we have dissected the mechanism by which SOX7 regulates the emergence of hematopoietic cells from HE in the yolk sac. We uncovered that SOX7 inhibits the expression of genes positively regulated by RUNX1 and TAL1, while having no effect on the expression of these key transcriptional regulators. Furthermore, we demonstrate that SOX7 can strongly inhibit the transcriptional activity of RUNX1 and transcriptional complexes containing RUNX1. The mechanism described herein for SOX7 therefore contrasts with that proposed for SOX17 in HE. Lizama and colleagues showed that SOX17 inhibits EHT by binding to the *Runx1* locus and repressing *Runx1* transcription (Lizama et al., 2015). It is interesting to speculate therefore that there is multi-layered regulation of RUNX1 in HE by SOX factors: SOX17 at the transcriptional level and SOX7 at the protein level. Another possibility, given the similarity of the HMG domain between the three SOXF factors (Bowles et al., 2000), is that SOX17 and SOX18 can also physically interact with RUNX1, although this remains to be proven.

Several studies have demonstrated that SOX17 expression during endothelial differentiation is restricted to arteries (Corada et al., 2013; Frame et al., 2015; Matsui et al., 2006). By contrast, SOX7 is

Development (2016) 143, 4341-4351 doi:10.1242/dev.140970

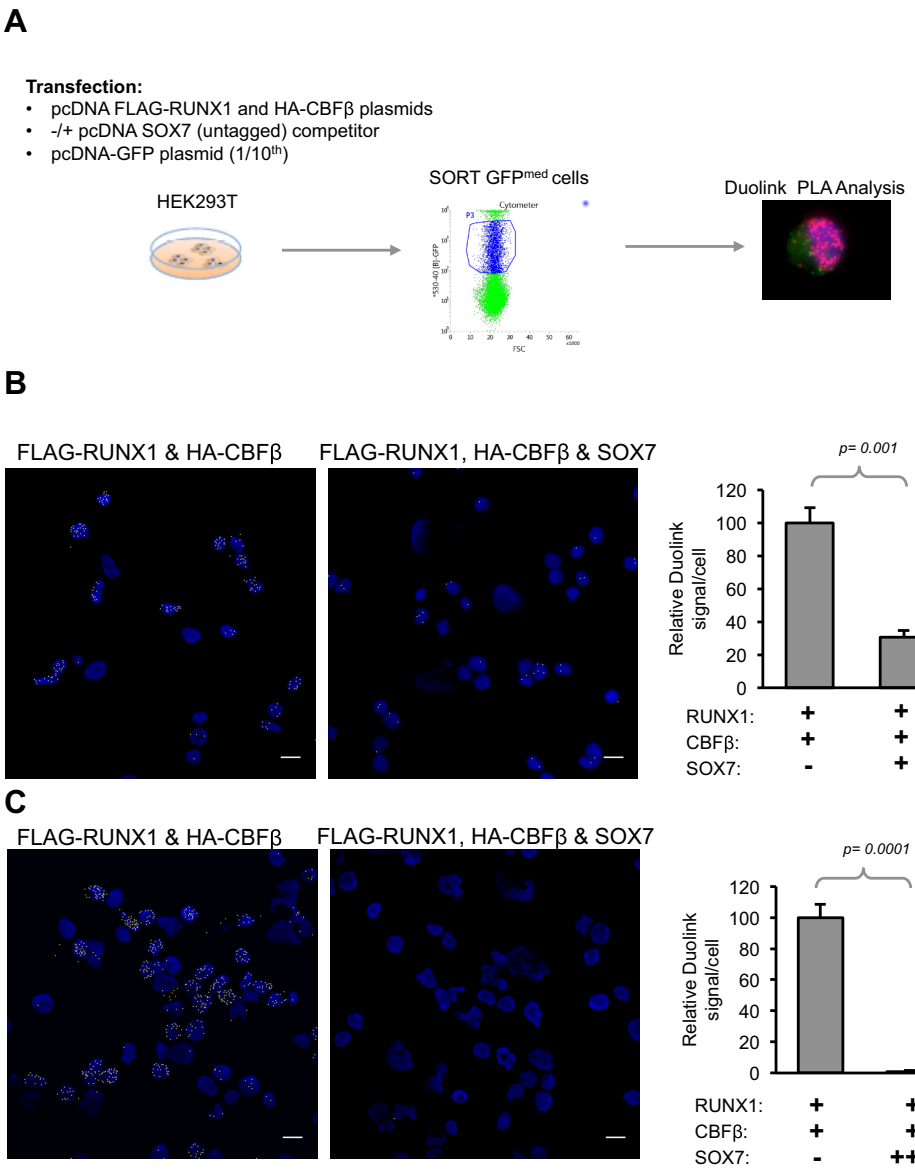

Fig. 6. SOX7 inhibits RUNX1 interaction with CBFβ. (A) HEK293T cells were transfected with pcDNA3 FLAG-RUNX1 and HA-CBFβ plasmids, with or without untagged SOX7 competitor, and pcDNA3-GFP plasmid. Transfected cells were enriched by sorting for GFP before subsequent Duolink PLA analysis. (B) RUNX1, CBFβ and SOX7 plasmids were transfected at equal concentration (1 µg each). (C) SOX7 was transfected at a three times greater concentration (3 µg) than RUNX1 and CBFβ plasmids (1 µg each). Left panels: representative micrographs. Scale bars: 20 µm. Right panels: mean Duolink signal per cell±s.e.m. relative to RUNX1 and CBFβ only (n=5 fields of view analysed using Student's two-tailed t-test).

expressed from the onset of endothelial differentiation in the yolk sac at E7.5, and is expressed in arterial and venous vasculature (Gandillet et al., 2009; Sakamoto et al., 2007; Zhou et al., 2015). In agreement with these data, we discovered that SOX7 is more broadly expressed across the yolk sac HE at E8.5 compared with SOX17. Therefore, it is likely that SOX7 plays a more important role than SOX17 in yolk sac HE, especially before and during vascular remodelling and in smaller blood vessels. As we also detect RUNX and SOX7 co-expressing cells in the AGM region of the dorsal aorta at E9.5, it is likely that both SOX7 and SOX17 regulate RUNX1 behaviour in this context. The role of SOX18 has not yet been investigated in HE; however, given the partial redundancy and compensation between the SOXF factors during endothelial development, it will be an interesting topic for future study.

Collectively, our data presented here and previous studies demonstrate that SOX7 is expressed in HE but is rapidly switched off during EHT (Costa et al., 2012). The expression of the RUNX1b isoform is low in HE but it increases during EHT before the subsequent rapid upregulation of RUNX1c in emerging hematopoietic progenitors (Sroczynska et al., 2009a; Swiers et al., 2013). RUNX1 is a master regulator of EHT: activating the expression of hematopoietic genes, while switching off the endothelial transcriptional program via activation of GFI1 expression (Lancrin et al., 2012; Lie-A-Ling et al., 2014; Tanaka et al., 2012; Thambyrajah et al., 2016). We propose that in the early stages of HE differentiation, SOX7 can outcompete CBFβ for RUNX1 binding, while also preventing RUNX1 binding to its hematopoietic target genes (Fig. 7C). As the endothelial transcriptional program is switched off, SOX7 expression decreases and RUNX1 is free to interact with CBFβ and to bind its target sites, resulting in switching on of the hematopoietic transcriptional program (Fig. 7C). In this study, we therefore propose a novel model where the balance of protein interactions between opposing endothelial and hematopoietic transcription factors fine-tunes HE differentiation and temporally regulates the emergence of hematopoietic progenitors.

The mechanism by which SOX7 regulates hematopoietic differentiation by interacting with RUNX1 is strikingly similar to the roles of SOX9 and RUNX2 in osteo-chondrogenic differentiation (Akiyama et al., 2005; Zhou et al., 2006). In this scenario, SOX9 inhibits RUNX2 DNA binding and RUNX2 transcriptional activity, which promotes chondrogenesis (Zhou

Development (2016) 143, 4341-4351 doi:10.1242/dev.140970

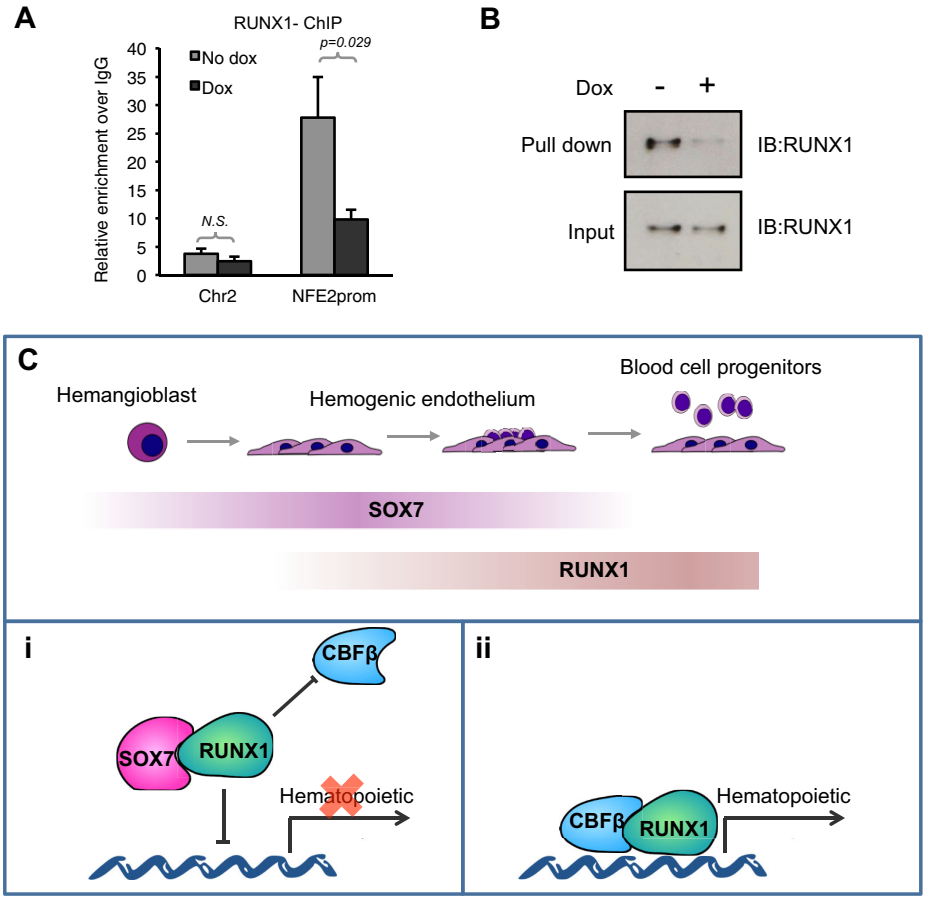

Fig. 7. SOX7 inhibits RUNX1 DNA binding. (A) CD41$^+$ cells were sorted from *iSox7* EBs and cultured for 12 h with and without doxycycline before ChIP analysis. Data are presented as mean±s.e.m., n=4 independent experiments analysed using Student's one-tailed t-test. (B) Biotin-DNA pull-down analysis of RUNX1 DNA binding. Nuclear extracts from above CD41$^+$ cells were incubated with a biotin-labelled DNA sequence containing a RUNX1-binding site before pull-down and immunoblotting. (C) Model of the balance between SOX7 and RUNX1, which controls the emergence of hematopoietic cells. (i) SOX7 can outcompete CBFβ for RUNX1 binding, preventing RUNX1 binding to its hematopoietic target genes. (ii) As the endothelial program is switched off, SOX7 expression decreases and RUNX1 is free to interact with CBFβ, to bind its target sites and to activate the hematopoietic program.

et al., 2006). However, in progenitors expressing low levels of SOX9, RUNX2 is free to promote osteogenesis (Zhou et al., 2006). Consequently, the balance between SOX9 and RUNX2 regulates the cell fate decisions of osteo-chondrogenic progenitors. It will be interesting to investigate whether interplay between SOX and RUNX factors is an important developmental mechanism for regulating cell fate decisions during differentiation of other cell lineages.

MATERIALS AND METHODS

Embryonic stem cell (ESC) culture and differentiation

ESCs were cultured and differentiated as previously described (Sroczynska et al., 2009b). Embryoid bodies (EBs) were routinely maintained up to day 3.5, and FLK1$^+$ cells were isolated and cultured as previously described for HE differentiation (Fehling et al., 2003; Lancrin et al., 2009). The *iSox7* cell line was generated as previous described (Costa et al., 2012), authenticated and regularly checked for contamination. Doxycycline was added to cultures at 1 µg/ml where indicated.

Hematopoietic progenitor cell CFU assays

Differentiating HE cultures were replated into methylcellulose-based hematopoietic progenitor cell differentiation media as previously described (Gandillet et al., 2009; Sroczynska et al., 2009b). Doxycycline was added at 1 µg/ml where indicated; primitive erythroid colonies were scored on day 4 and definitive colonies were scored on day 8. At the end of the culture period, colonies were harvested and analysed for hematopoietic differentiation by flow cytometry.

Hematopoietic differentiation of yolk sac explants and cell suspensions

E9.5 yolk sac explants were cultured for 2 days in explant medium adapted from Malik et al. (2013), containing: IMDM, 16% BIT serum substitute (Stem Cell Technologies), 50 µg/ml ascorbic acid (Sigma), 0.5% PFHMII (Invitrogen), 15% serum replacement (Invitrogen), 5% platelet-derived serum, 2 mM L-glutamine (Gibco), 150 µM MTG (Sigma), 2 U/ml EPO (Eprex, Janssen-Cilag) and 100 ng/ml SCF (Peprotech) (protocol kindly provided by Professor James Palis, University of Rochester Medical Center, Rochester, USA). For dissociated yolk sac cultures, E9.5 yolk sacs were dissociated with collagenase dispase (Roche) diluted to 1 mg/ml in PBS for 20 min at 37°C. Yolk sac cell suspensions were cultured for 4 days on OP9 cells in HE differentiation media previously described for AGM culture (Thambyrajah et al., 2016). Doxycycline was added to all yolk sac cultures at 1 µg/ml.

Mouse lines

Targeted *Sox7* ESC clone B9 (International Knockout Mouse Consortium) was injected into mouse blastocysts. Resultant chimaeras were crossed with C57BL/6 mice. Subsequent generations were crossed with PGK-Cre mice to excise the neomycin cassette and the critical exon 2 of the *Sox7* gene, resulting in the generation of a LacZ-tagged null allele (*Sox7*$^{-/+}$). The *Runx1b::rfp* transgenic line was generated as previously described (Sroczynska et al., 2009a), except that the hCD4 reporter was replaced with RFP. The *iSox7* transgenic line was generated as previously described (Gandillet et al., 2009).

Timed matings

Timed matings were set up between: male and female *Sox7*$^{-/+}$ mice, male *Runx1*$^{RFP/WT}$ and female *ICR*$^{WT/WT}$ mice and between male *iSox7*$^+$/*rtTA*$^+$ and female *ICR*$^{WT/WT}$ mice. The morning of vaginal plug detection was embryonic day (E) 0.5. All animal work was performed under regulation governed by the UK Home Office Legislation under the Animal Scientific Procedures Act (ASPA) 1986.

Duolink proximity ligation assay (PLA)

HEK293T cells were seeded at 2×10^6 cells/plate in a 100 mm plate containing IMDM 10% FBS media. The following day, cells were

Development (2016) 143, 4341-4351 doi:10.1242/dev.140970

transfected using gene juice (Novagen) according to the manufacturer's instructions, with 2 µg of each of the pcDNA-transcription factor plasmids and 200 ng of pcDNA-GFP plasmid. After 48 h, GFP^+ cells were sorted and 1×10^4 cells were attached to microscope slides by cytospsin before fixation with 4% PFA and permeabilisation with 0.3% Triton X-100. Subsequent steps were performed using the Duolink PLA red detection kit, according to the manufacturer's instructions (Sigma). For competitive interaction assays, HEK293T cells were transfected either with equal amounts of each plasmid (1 µg each) or with the competitor plasmid (3 µg) at three times the concentration of the other plasmids (1 µg each). A GFP (200 ng)-expressing plasmid was used to enrich for transfected cells for both transfections, and the rest of the steps were carried out as above.

Duolink images were analysed using Image J software. The nuclear DAPI channel images were overlaid with binary Duolink puncta images and protein interactions were quantified by counting the number of Duolink puncta per nucleus for each cell in the field of view.

Whole-mount staining

Embryos were stained as previously described (Yokomizo et al., 2013) using a goat anti-SOX7 antibody (1:200) (R&D systems; AF2766) and a donkey anti-goat AF647 antibody (1:2000) (Invitrogen; A-21447). Subsequently, embryos were incubated with a rat anti-CD31 antibody (1:1000) (BD Biosciences; 553370) and a rabbit anti-pan-RUNX antibody (1:1000) (Abcam; ab92336) before staining with a goat anti-rat AF488 and a goat anti-rabbit antibody (both 1:2000) (both Invitrogen). Yolk sacs were isolated and flat mounted with DAPI, as previously described (Frame et al., 2015), before imaging. All primary antibodies have been used in previous studies (Yokomizo et al., 2013; Yzaguirre and Speck, 2016; Zhou et al., 2015). Specific labelling of primary antibodies was determined by comparison with no primary antibody-treated controls.

Luciferase assays

All assays were performed using the Dual-Luciferase Reporter System (Promega) and luciferase activities were measured with the GloMax-Multi Detection System (Promega) according to the manufacturer's instructions. The osteocalcin 6×OSE2-luc RUNX luciferase reporter has been described previously (Zhou et al., 2006).

RNAseq analysis

RNA was isolated from sorted $FLK1^+$ cells cultured for 48 h in HE media before pulsing with or without 1 µg/ml of doxycycline for 6, 12 and 24 h. Indexed polyA libraries were prepared using 200 ng of total RNA and 14 cycles of amplification in the Agilent Sure Select Automated Strand Specific RNA library prep for Illumina Multiplexed sequencing (G9691-90030) on an Agilent Bravo-BenchCel-MiniHub Automated Liquid Handling Platform. Libraries were sized on an Agilent Bioanalyzer (G2940CA) using a High Sensitivity DNA Kit (5067-4626) and quantified by qPCR using a Kapa Library Quantification Kit for Illumina sequencing platforms (KK4835). Pooled libraries were sequenced at 1×75 bp on an Illumina NextSeq500 system (SY-415-1001).

Single end sequencing (75 bp) were aligned to the mouse reference genome GRCm38 (Ensembl v76) using Bowtie2 (version 2.2.1) with default settings. Lane-wise and technical replicates of the same samples were merged into one BAM file. The expression levels of 41,228 annotated features were determined using the feature Counts function from the Bioconductor package Rsubread (version 1.13.13).

The Bioconductor package edgeR (version 3.8.5) was used to identify genes that showed statistically significant variation in expressions level in the following doxycycline treatment. The data were filtered to include only genes with at least 1 count-per-million reads and differential expression analysis was performed using the function exactTest in edgeR. Genes differentially expressed 1.5-fold following doxycycline treatment (P-value <0.05, FDR<0.1) are shown.

Single-cell qPCR

Single $RUNX1\text{-}RFP^+/FLK1^+/CD41^-$ cells were sorted from E8.5 $RUNX1^{RFP/WT}$ embryos, then cDNA synthesis and specific target amplification (STA) was performed as previously described (Moignard et al., 2013). Single-cell qPCR was performed with 1 µl of STA mix (diluted 5 fold), 0.1 µM probes from the universal probe library (Roche), 0.2 µM primers (see Table S4) and 1× TaqMan master mix (Applied Biosystems). The number of cells expressing each SOXF factor above the limit of detection was calculated.

QPCR

$FLK1^+/CD41^-$ HE enriched cells were sorted from $SOX7^{-/-}$ and $SOX7^{+/+}$ E8.5 embryos and total RNA was isolated using an RNeasy Micro plus Kit (Qiagen) according to the manufacturer's instructions. cDNA synthesis and STA was performed using 1 µl of isolated RNA, and qPCR was performed as above using 1 µl STA mix (diluted 1000-fold). Gene expression was calculated relative to β-actin using the ΔΔCt method.

RUNX1 ChIP

$FLK1^+$ cells were sorted from *iSox7* EBs, reaggregated and cultured for 2 days (as described previously) to generate HPCs (Goode et al., 2016). $CD41^+$ cells were sorted and cultured with or without 1 µg/ml doxycycline for 12 h, before harvesting. Chromatin immunoprecipitation was performed using the HighCell# ChIP kit (Diagenode) according to the manufacturer's instructions. Briefly, cells were crosslinked for 8 min in 1% formaldehyde and the nuclei were then sonicated for 15 cycles (30 s on/30 s off) with the Bioruptor (Diagenode). Five-million cells were used for each immunoprecipitation with either the control immunoglobulin or the anti-RUNX1 antibody (4 µg) (Abcam). RUNX1 binding to the *Nfe2* promoter was assessed by SYBR green qPCR using 0.25 µM primers (see Table S4) and 1×SYBR green mix. For data analysis, ChIP signals were normalised first to input then to IgG reference levels.

Biotin-DNA pull-down

Biotin-DNA pull-down assays were performed as previously described (Costa et al., 2012), using a biotinylated 30 bp probe taken from the osteocalcin promoter containing a single RUNX-binding site (see Table S4 for sequence).

Flow cytometry and FACs

Cells were dissociated by trypsinisation, washed with IMDM media containing 10% FBS and stained with the following antibodies for 30 min on ice: CD41 PE/Cy7 (1:400), CD41 APC (1:400), CD45 PerCP-Cy5.5 (1:200), cKIT APC eflour780 (1:200), TIE2 PE (1:200) (all eBioscience) and FLK1-PE/Cy7 (1:300) (Biolegend). Cells were washed and analysed using an LSRII flow cytometer (BD) or sorted on an ARIAIII FACs machine (BD). Subsequent analysis was performed using FlowJo software V9 (Tree Star), gating first on the viable cells from the forward and side scatter.

Statistics

Sample sizes were chosen based on pilot studies. Student's t-test was used to assess the differences between two populations in both cell line and embryo experiments. A hypergeometric probability test was used to assess the significance of overlap between two gene lists. Chi-squared test was used to assess frequency differences between single cell populations. $*P<0.05$, $**P<0.01$, $***P<0.001$.

Acknowledgements

We thank Professor James Palis for provision of the yolk sac flat mounting and yolk sac explant culture protocols. We thank the staff at the Flow Cytometry, Advanced Imaging and Molecular Biology Core facilities of CRUK Manchester Institute for technical support.

Competing interests

The authors declare no competing or financial interests.

Author contributions

A.J.L. designed and performed experiments, analysed the data and wrote the manuscript. G.C. and A.L. designed and performed experiments. M.Z.H.F. performed bioinformatics analysis on the sequencing data. M.L.-A-L. designed experiments. G.L. and V.K. designed and supervised the research project, analysed the data, and wrote the manuscript.

Funding
This work is supported by Cancer Research UK [core grant to CRUK MI] and the Biotechnology and Biological Sciences Research Council [BB/I001794/1].

Data availability
The GEO accession number for the RNAseq data is GSE81466.

Supplementary information
Supplementary information available online at
http://dev.biologists.org/lookup/doi/10.1242/dev.140970.supplemental

References

Akiyama, H., Kim, J.-E., Nakashima, K., Balmes, G., Iwai, N., Deng, J. M., Zhang, Z., Martin, J. F., Behringer, R. R. Nakamura, T. et al. (2005). Osteo-chondroprogenitor cells are derived from Sox9 expressing precursors. *Proc. Natl. Acad. Sci. USA* **102**, 14665-14670.

Bos, F. L., Hawkins, J. S. and Zovein, A. C. (2015). Single-cell resolution of morphological changes in hemogenic endothelium. *Development* **142**, 2719-2724.

Bowles, J., Schepers, G. and Koopman, P. (2000). Phylogeny of the SOX family of developmental transcription factors based on sequence and structural indicators. *Dev. Biol.* **227**, 239-255.

Chen, M. J., Yokomizo, T., Zeigler, B. M., Dzierzak, E. and Speck, N. A. (2009). Runx1 is required for the endothelial to haematopoietic cell transition but not thereafter. *Nature* **457**, 887-891.

Corada, M., Orsenigo, F., Morini, M. F., Pitulescu, M. E., Bhat, G., Nyqvist, D., Breviario, F., Conti, V., Briot, A. and Iruela-Arispe, M. L. et al. (2013). Sox17 is indispensable for acquisition and maintenance of arterial identity. *Nat. Commun.* **4**, 2609.

Costa, G., Mazan, A., Gandillet, A., Pearson, S., Lacaud, G. and Kouskoff, V. (2012). SOX7 regulates the expression of VE-cadherin in the haemogenic endothelium at the onset of haematopoietic development. *Development* **139**, 1587-1598.

Fehling, H. J., Lacaud, G., Kubo, A., Kennedy, M., Robertson, S., Keller, G. and Kouskoff, V. (2003). Tracking mesoderm induction and its specification to the hemangioblast during embryonic stem cell differentiation. *Development* **130**, 4217-4227.

Frame, J. M., Fegan, K. H., Conway, S. J., McGrath, K. E. and Palis, J. (2015). Definitive hematopoiesis in the yolk sac emerges from Wnt-responsive hemogenic endothelium independently of circulation and arterial identity. *Stem Cells* **34**, 431-444.

Gandillet, A., Serrano, A. G., Pearson, S., Lie, A.-L. M., Lacaud, G. and Kouskoff, V. (2009). Sox7-sustained expression alters the balance between proliferation and differentiation of hematopoietic progenitors at the onset of blood specification. *Blood* **114**, 4813-4822.

Goode, D. K., Obier, N., Vijayabaskar, M. S., Lie-A-Ling, M., Lilly, A. J., Hannah, R., Lichtinger, M., Batta, K., Florkowska, M. and Patel, R. et al. (2016). Dynamic gene regulatory networks drive hematopoietic specification and differentiation. *Dev. Cell* **36**, 572-587.

Huang, G., Shigesada, K., Ito, K., Wee, H.-J., Yokomizo, T. and Ito, Y. (2001). Dimerization with PEBP2beta protects RUNX1/AML1 from ubiquitin-proteasome-mediated degradation. *EMBO J.* **20**, 723-733.

Lancrin, C., Sroczynska, P., Stephenson, C., Allen, T., Kouskoff, V. and Lacaud, G. (2009). The haemangioblast generates haematopoietic cells through a haemogenic endothelium stage. *Nature* **457**, 892-895.

Lancrin, C., Mazan, M., Stefanska, M., Patel, R., Lichtinger, M., Costa, G., Vargel, O., Wilson, N. K., Moroy, T. and Bonifer, C. et al. (2012). GFI1 and GFI1B control the loss of endothelial identity of hemogenic endothelium during hematopoietic commitment. *Blood* **120**, 314-322.

Landry, J.-R., Kinston, S., Knezevic, K., de Bruijn, M. F. T. R., Wilson, N., Nottingham, W. T., Peitz, M., Edenhofer, F., Pimanda, J. E. and Ottersbach, K. et al. (2008). Runx genes are direct targets of Scl/Tal1 in the yolk sac and fetal liver. *Blood* **111**, 3005-3014.

Lie-A-Ling, M., Marinopoulou, E., Li, Y., Patel, R., Stefanska, M., Bonifer, C., Miller, C., Kouskoff, V. and Lacaud, G. (2014). RUNX1 positively regulates a cell adhesion and migration program in murine hemogenic endothelium prior to blood emergence. *Blood* **124**, e11-e20.

Lilly, A. J., Lacaud, G. and Kouskoff, V. (2016). SOXF transcription factors in cardiovascular development. *Semin. Cell Dev. Biol.* pii: S1084-9521(16)30216-6.

Link, K. A., Chou, F.-S. and Mulloy, J. C. (2010). Core binding factor at the crossroads: determining the fate of the HSC. *J. Cell. Physiol.* **222**, 50-56.

Lizama, C. O., Hawkins, J. S., Schmitt, C. E., Bos, F. L., Zape, J. P., Cautivo, K. M., Borges Pinto, H., Rhyner, A. M., Yu, H. and Donohoe, M. E. et al. (2015). Repression of arterial genes in hemogenic endothelium is sufficient for haematopoietic fate acquisition. *Nat. Commun.* **6**, 7739.

Malik, J., Kim, A. R., Tyre, K. A., Cherukuri, A. R. and Palis, J. (2013). Erythropoietin critically regulates the terminal maturation of murine and human primitive erythroblasts. *Haematologica* **98**, 1778-1787.

Matsui, T., Kanai-Azuma, M., Hara, K., Matoba, S., Hiramatsu, R., Kawakami, H., Kurohmaru, M., Koopman, P. and Kanai, Y. (2006). Redundant roles of Sox17 and Sox18 in postnatal angiogenesis in mice. *J. Cell Sci.* **119**, 3513-3526.

Moignard, V., Macaulay, I. C., Swiers, G., Buettner, F., Schütte, J., Calero-Nieto, F. J., Kinston, S., Joshi, A., Hannah, R. and Theis, F. J. et al. (2013). Characterization of transcriptional networks in blood stem and progenitor cells using high-throughput single-cell gene expression analysis. *Nat. Cell Biol.* **15**, 363-372.

Moignard, V., Woodhouse, S., Haghverdi, L., Lilly, A. J., Tanaka, Y., Wilkinson, A. C., Buettner, F., Macaulay, I. C., Jawaid, W. and Diamanti, E. et al. (2015). Decoding the regulatory network of early blood development from single-cell gene expression measurements. *Nat. Biotechnol.* **33**, 269-276.

North, T., Gu, T. L., Stacy, T., Wang, Q., Howard, L., Binder, M., Marin-Padilla, M. and Speck, N. A. (1999). Cbfa2 is required for the formation of intra-aortic hematopoietic clusters. *Development* **126**, 2563-2575.

Otto, F., Thornell, A. P., Crompton, T., Denzel, A., Gilmour, K. C., Rosewell, I. R., Stamp, G. W. H., Beddington, R. S. P., Mundlos, S. and Olsen, B. R. et al. (1997). Cbfa1, a candidate gene for cleidocranial dysplasia syndrome, is essential for osteoblast differentiation and bone development. *Cell* **89**, 765-771.

Sakamoto, Y., Hara, K., Kanai-Azuma, M., Matsui, T., Miura, Y., Tsunekawa, N., Kurohmaru, M., Saijoh, Y., Koopman, P. and Kanai, Y. (2007). Redundant roles of Sox17 and Sox18 in early cardiovascular development of mouse embryos. *Biochem. Biophys. Res. Commun.* **360**, 539-544.

Solaimani Kartalaei, P., Yamada-Inagawa, T., Vink, C. S., de Pater, E., van der Linden, R., Marks-Bluth, J., van der Sloot, A., van den Hout, M., Yokomizo, T. and van Schaick-Solernó, M. L. et al. (2015). Whole-transcriptome analysis of endothelial to hematopoietic stem cell transition reveals a requirement for Gpr56 in HSC generation. *J. Exp. Med.* **212**, 93-106.

Sroczynska, P., Lancrin, C., Kouskoff, V. and Lacaud, G. (2009a). The differential activities of Runx1 promoters define milestones during embryonic hematopoiesis. *Blood* **114**, 5279-5289.

Sroczynska, P., Lancrin, C., Pearson, S., Kouskoff, V. and Lacaud, G. (2009b). In vitro differentiation of mouse embryonic stem cells as a model of early hematopoietic development. *Methods Mol. Biol.* **538**, 317-334.

Swiers, G., Baumann, C., O'Rourke, J., Giannoulatou, E., Taylor, S., Joshi, A., Moignard, V., Pina, C., Bee, T. and Kokkaliaris, K. D. et al. (2013). Early dynamic fate changes in haemogenic endothelium characterized at the single-cell level. *Nat. Commun.* **4**, 2924.

Tanaka, Y., Joshi, A., Wilson, N. K., Kinston, S., Nishikawa, S. and Göttgens, B. (2012). The transcriptional programme controlled by Runx1 during early embryonic blood development. *Dev. Biol.* **366**, 404-419.

Thambyrajah, R., Mazan, M., Patel, R., Moignard, V., Stefanska, M., Marinopoulou, E., Li, Y., Lancrin, C., Clapes, T. and Möröy, T. et al. (2016). GFI1 proteins orchestrate the emergence of haematopoietic stem cells through recruitment of LSD1. *Nat. Cell Biol.* **18**, 21-32.

Wang, S., Wang, Q., Crute, B. E., Melnikova, I. N., Keller, S. R. and Speck, N. A. (1993). Cloning and characterization of subunits of the T-cell receptor and murine leukemia virus enhancer core-binding factor. *Mol. Cell. Biol.* **13**, 3324-3339.

Wilson, N. K., Foster, S. D., Wang, X., Knezevic, K., Schütte, J., Kaimakis, P., Chilarska, P. M., Kinston, S., Ouwehand, W. H. and Dzierzak, E. et al. (2010). Combinatorial transcriptional control in blood stem/progenitor cells: genome-wide analysis of ten major transcriptional regulators. *Cell Stem Cell* **7**, 532-544.

Wright, E. M., Snopek, B. and Koopman, P. (1993). Seven new members of the Sox gene family expressed during mouse development. *Nucleic Acids Res.* **21**, 744.

Yokomizo, T., Yamada-Inagawa, T., Yzaguirre, A. D., Chen, M. J., Speck, N. A. and Dzierzak, E. (2013). Whole-mount three-dimensional imaging of internally localized immunostained cells within mouse embryos. *Nat. Protoc.* **7**, 421-431.

Yzaguirre, A. D. and Speck, N. A. (2016). Extravascular endothelial and hematopoietic islands form through multiple pathways in midgestation mouse embryos. *Dev. Biol.* **415**, 111-121.

Zhang, L., Lukasik, S. M., Speck, N. A. and Bushweller, J. H. (2003). Structural and functional characterization of Runx1, CBF beta, and CBF beta-SMMHC. *Blood Cells Mol. Dis.* **30**, 147-156.

Zhou, G., Zheng, Q., Engin, F., Munivez, E., Chen, Y., Sebald, E., Krakow, D. and Lee, B. (2006). Dominance of SOX9 function over RUNX2 during skeletogenesis. *Proc. Natl. Acad. Sci. USA* **103**, 19004-19009.

Zhou, Y., Williams, J., Smallwood, P. M. and Nathans, J. (2015). Sox7, Sox17, and Sox18 cooperatively regulate vascular development in the mouse retina. *PLoS ONE* **10**, e0143650.

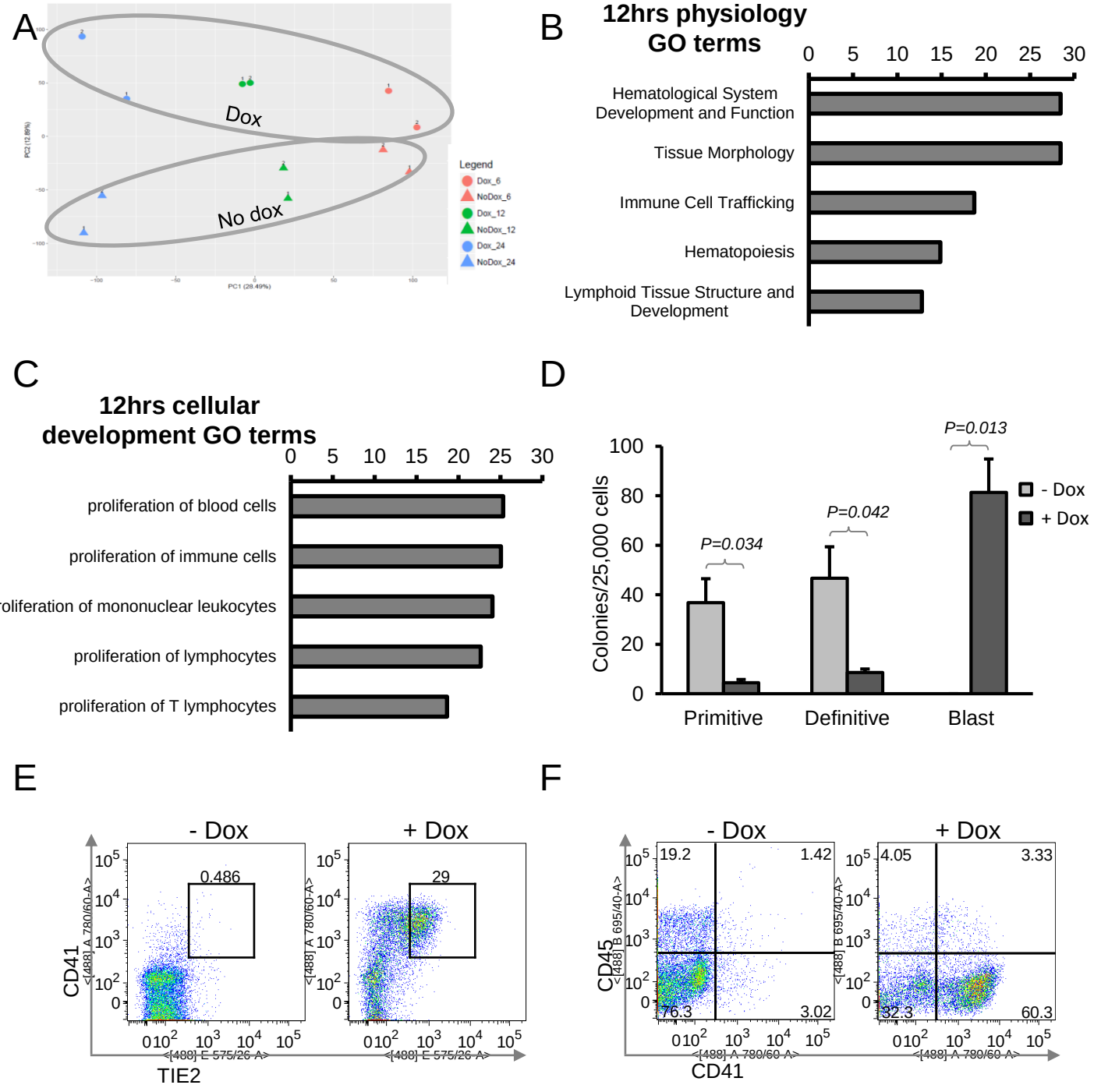

Figure S1. SOX7 inhibits a hematopoietic transcriptional program. FLK1^{+} cells were sorted from day 3.5 *iSox7* EBs and cultured in HE differentiation media. Doxycycline was added after 48 hours, and RNAseq was performed 6, 12 and 24 hours post doxycycline induction. Cells were replated in a hematopoietic progenitor cell CFU assay 24 hours post doxycycline induction. (A) PCA plot of RNAseq dataset at 6, 12, and 24 hours post doxycycline induction. (B & C) Ingenuity Pathway Analysis of the genes inhibited by SOX7 at 12 hours. (D) Hematopoietic progenitor cell CFU assay with and without doxycycline (n=3 biological repeats, Student's one-tailed paired t-test). (E & F) Cells were harvested from the CFU assay after 8 days and analysed by flow cytometry.

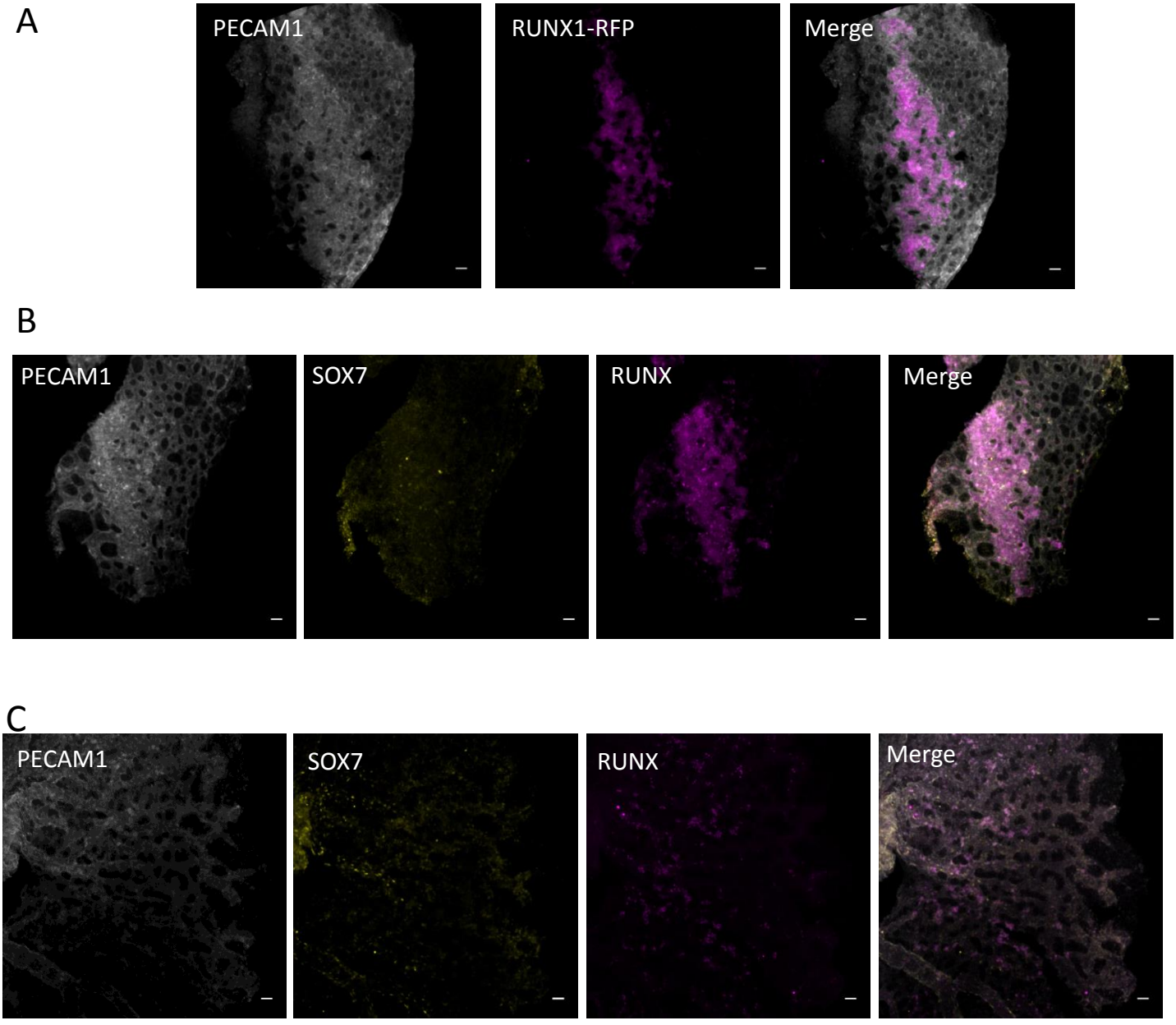

Figure S2. SOX7 and RUNX expression in the yolk sac at E8.5 and E9.5 (A) Wholemount staining for PECAM1 together with proximal RUNX1-RFP expression at E8.5 from RUNX1$^{RFP/WT}$ embryos. (B) Wholemount staining for SOX7, RUNX and PECAM1 in yolk sacs at E8.5. (C) Wholemount staining for SOX7, RUNX and PECAM1 in yolk sacs at E9.5. Scale bars 50µm (A & B), 20µm (C).

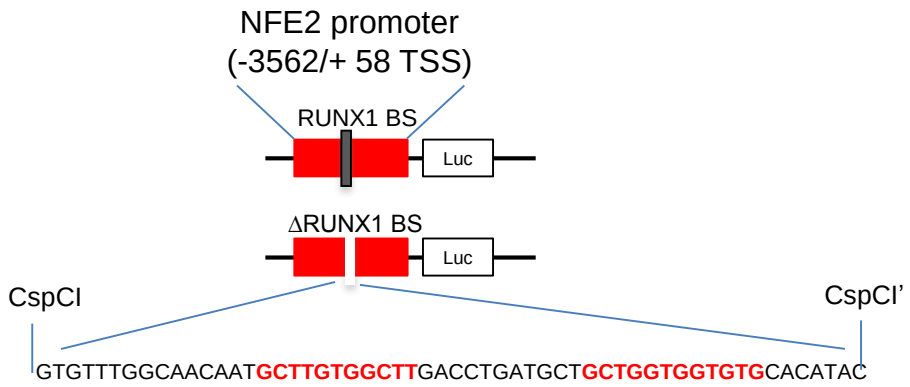

Figure S3. RUNX1 binds the NFE2 promoter region. (A) Deletion of two RUNX1 binding sites (red) in the NFE2 promoter using CspCI restriction enzyme.

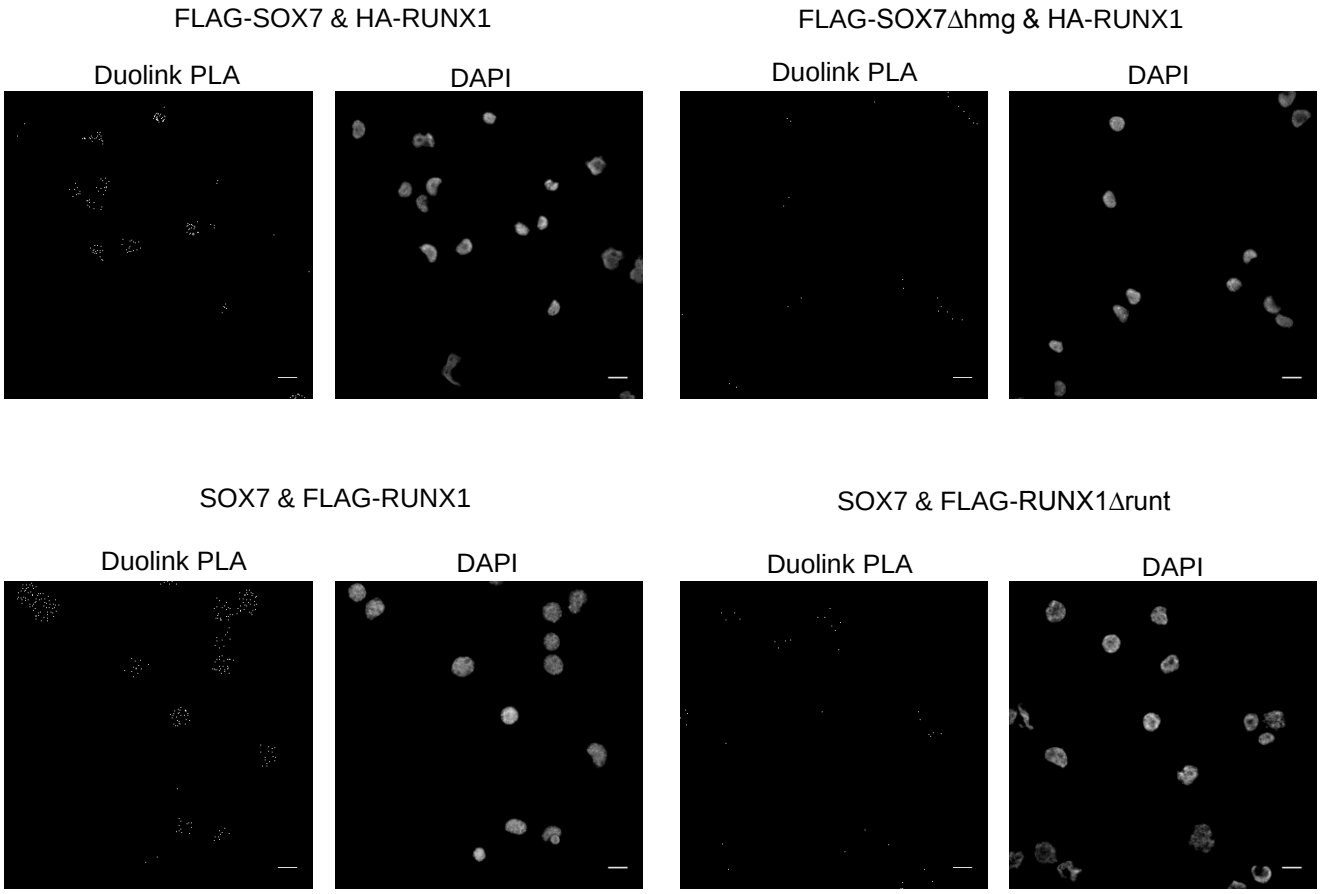

Figure S4. Single channel images of the representative Duolink PLA in Figure 5. HEK293T cells were transfected with the indicated pcDNA3 plasmids before Duolink PLA. Scale bars: 20μm.

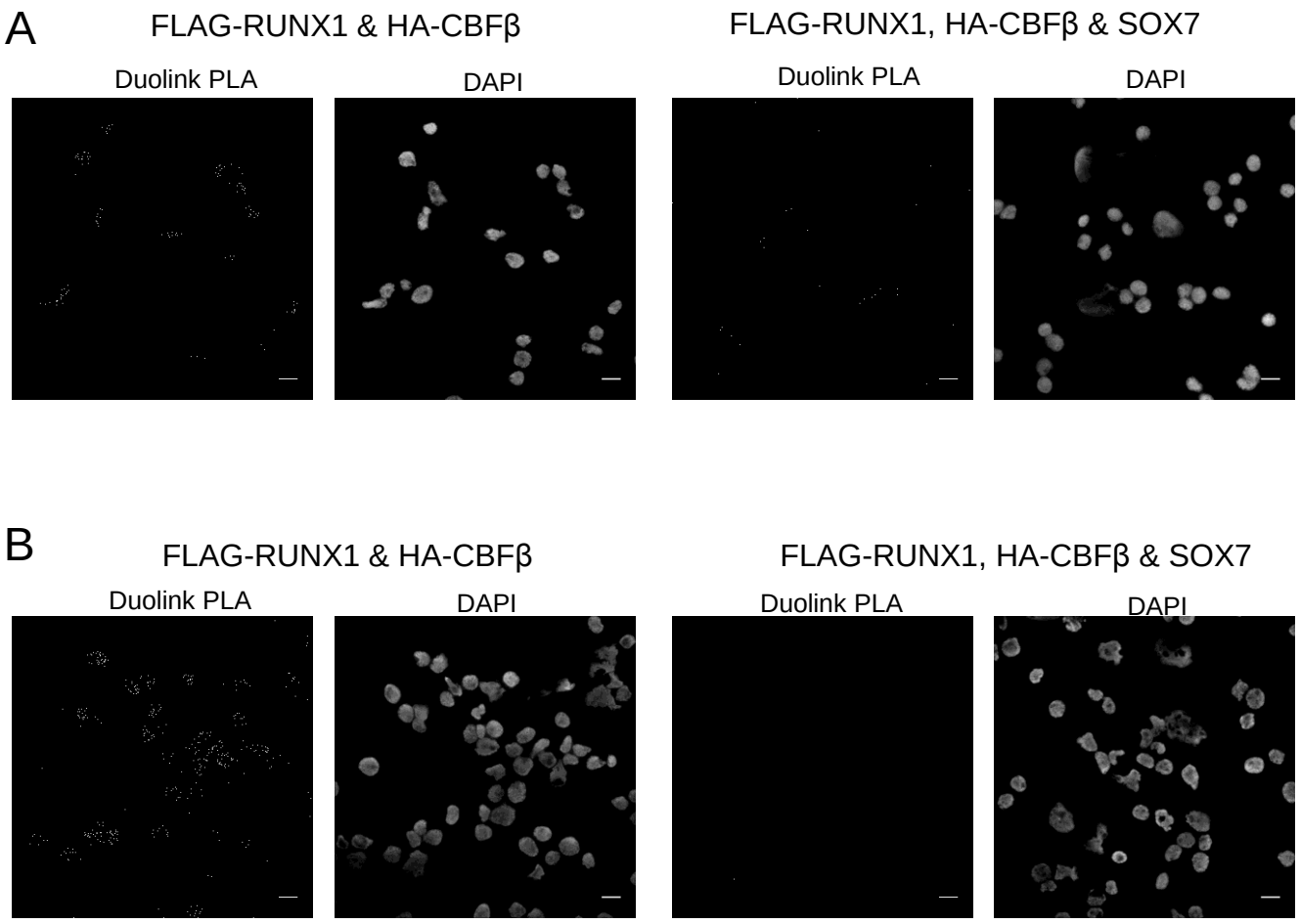

Figure S5. Single channel images of representative Duolink PLA in Figure 6. (A) RUNX1, CBFβ and SOX7 plasmids were transfected at equal concentration (1µg each). (B) SOX7 was transfected at 3 times greater concentration (3µg) than RUNX1 and CBFβ plasmids (1µg each). Scale bars: 20µm.

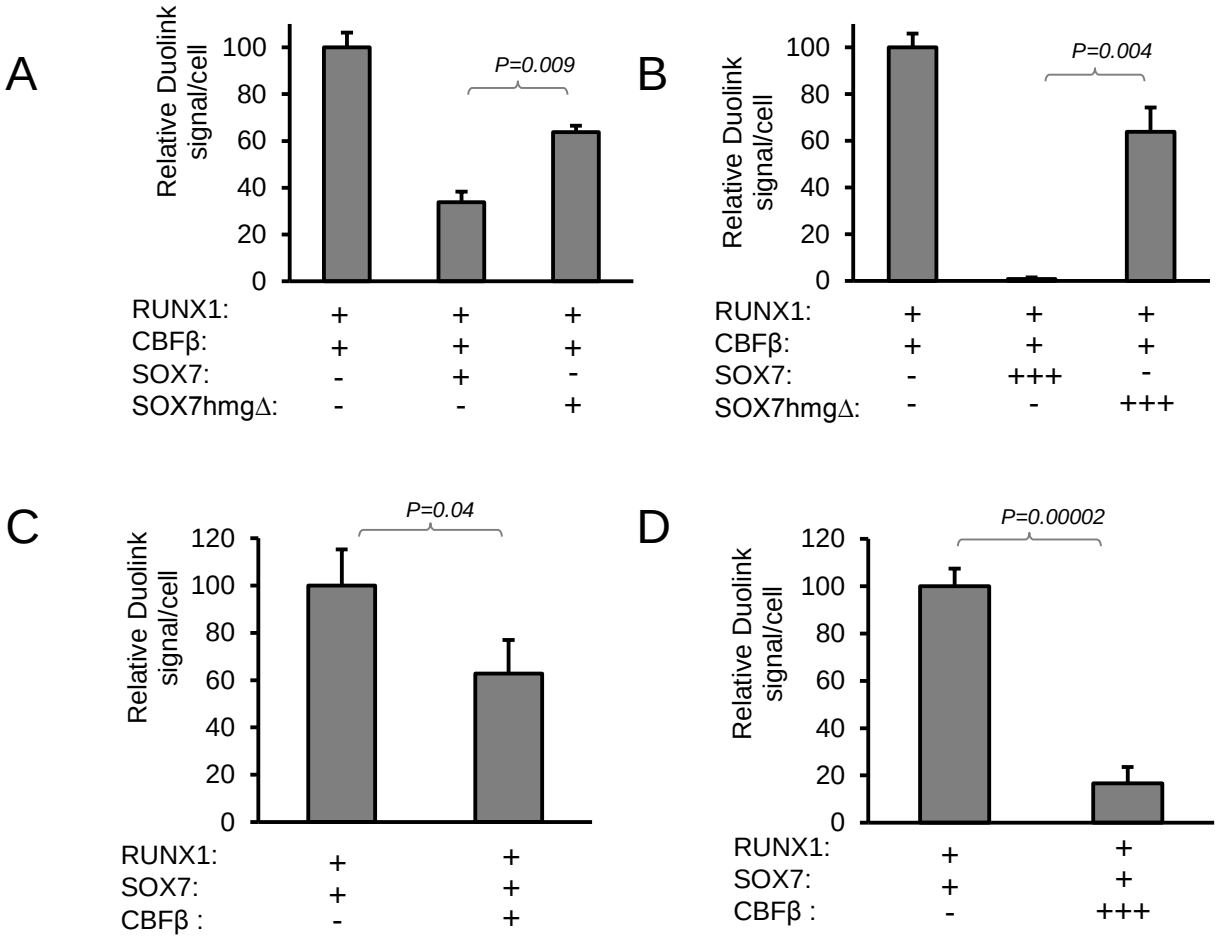

Figure S6. Competition between SOX7 and CBFβ for RUNX1 binding. HEK293T cells were transfected with pcDNA3 RUNX1, CBFβ, SOX7 and SOX7hmgΔ plasmids as indicated, together with a pcDNA3-GFP plasmid. Transfected cells were enriched by sorting for GFP before subsequent Duolink PLA analysis. (A & B) Duolink PLA analysis between RUNX1 and CBFβ, with SOX7/SOX7hmgΔ added as competitor. (A) plasmids were transfected at equal concentration (1µg each plasmid). (B) SOX7/SOX7hmgΔ plasmids were transfected at a 3 times greater concentration (3µg) than RUNX1 and CBFβ plasmids (1µg each). (C & D) Duolink PLA analysis between RUNX1 and SOX7, with CBFβ added as a competitor. (C) RUNX1, SOX7 and CBFβ plasmids were transfected at equal concentration (1µg each). (D) CBFβ plasmid was transfected at 3 times greater concentration (3µg) than RUNX1 and SOX7 plasmids (1µg each). All experiments are n=5, Student's two-tailed t-test.

Table S1. Differentially expressed genes at 6 hours, at least 1.5-fold change

Click here to Download Table S1

Table S2. Differentially expressed genes at 12 hours, at least 1.5-fold change

Click here to Download Table S2

Table S3. Differentially expressed genes at 24 hours, at least 1.5 fold change

Click here to Download Table S3

Table S4. List of PCR primers

Click here to Download Table S4